JPET Fast Forward. Published on September 1, 2005 as DOI: 10.1124/jpet.105.089763

JPET #89763

Modulation of cytochrome c oxidase-Va is possibly involved in metallothionein protection from doxorubicin cardiotoxicity

Kevyn E. Merten, Wenke Feng, Li Zhang, William Pierce, Jian Cai,

Jon B. Klein, and Y. James Kang

Departments of Pharmacology and Toxicology (K.E.M., W.P., J.C., Y.J.K.) and Medicine

(W.F., L.Z., J.B.K., Y.J.K), University of Louisville School of Medicine,

Louisville, Kentucky 40202

JPET Fast Forward. Published on September 6, 2005 as DOI: 10.1124/jpet.105.089763
This article has not been copyedited and formatted. The final version may differ from this version.

Running Title: CCO-Va and metallothionein cardioprotection

Correspondence and reprint request address: Dr. Y. James Kang
Department of Medicine
University of Louisville School of Medicine
511 S. Floyd St., MDR 530
Louisville, KY 40202
Telephone: (502) 852-8677
Fax: (502) 852-6904
yjkang01@louisville.edu

Number of text pages: 23

Tables: 1

Figures: 5

References: 25

Abstract word count: 223

Introduction word count: 425

Discussion word count: 870

Section assignment: Toxicology

Abbreviations: MT, metallothionein; DOX, doxorubicin; MT-TG, metallothionein-overexpressing transgenic; WT, non-transgenic wild-type; CCO, cytochrome c oxidase; CCO-Va, cytochrome c oxidase subunit Va; ROS, reactive oxygen species; MALDI-TOF, matrix-assisted laser desorption ionization time-of-flight; IEF, isoelectric focusing; IPG, immobilized pH gradient; PMF, peptide mass fingerprinting; α-CN, α-cyano-4- hydroxy-trans-cinnamic acid; NCBI, National Center for Biotechnology Information.

Abstract

Previous studies using a cardiac-specific metallothionein (MT)-overexpressing transgenic (MT-TG) mouse model have demonstrated that MT protects from doxorubicin (DOX)-induced oxidative heart injury. The molecular mechanisms that underlie this cardioprotection, however, have yet to be defined. In the present study, we tested the hypothesis that MT overexpression activates cytoprotective mechanisms leading to cardiac protection from DOX toxicity. MT-TG mice and non-transgenic wild-type (WT) controls were treated intraperitoneally with DOX at a single dose of 20 mg/kg and sacrificed on the third day after the treatment. An expression proteomic analysis involving two-dimensional gel electrophoresis and MALDI-TOF mass spectrometry was used to identify MT-induced changes in cytoprotection-related proteins. We identified 18 proteins that were modified by DOX treatment in the heart. These proteins included those involved in cellular antioxidant defense, enzymes of the mitochondrial electron transport chain, enzymes involved in β-oxidation of fatty acids and glycolysis, and proteins involved in regulation of cardiac muscle contraction. However, the most dominant modification by MT is the cytochrome c oxidase subunit Va (CCO-Va). In response to DOX treatment, a specific isoform of CCO-Va was enhanced in the MT-TG, but not in the WT mouse hearts. Since CCO-Va is a critical component in the mitochondrial electron transport chain, the results suggest that the cardioprotective effect of MT may be related to an increased expression or a differential modification of CCO-Va.

Introduction

Doxorubicin (DOX) is a valuable component of multiple chemotherapeutic regimens, however, severe cardiotoxicity is a major limiting factor that compromises its clinical use (Ferrans, 1978). Previous studies using a cardiac-specific metallothionein (MT)-overexpressing transgenic (MT-TG) mouse model have demonstrated that MT protects from DOX-induced oxidative cardiac injury (Kang et al., 1997; 2000; Sun et al., 2001). MT overexpression significantly inhibits DOX-induced apoptosis in the transgenic myocardium both *in vivo* (Kang et al., 2000) and *in vitro* (Wang et al., 2001a). Furthermore, MT prevents DOX-induced myocardial apoptosis via inhibition of DOX-activated p38 mitogen-activated protein kinase (MAPK) (Kang et al., 2000) and mitochondrial cytochrome c release and caspase-3 activation (Wang et al., 2001a). Studies using primary cultures of neonatal mouse cardiomyocytes have shown that DOX-generated reactive oxygen species (ROS) accumulate predominantly in the mitochondria (Wang et al., 2001a). MT eliminated the accumulation of ROS in the mitochondria (Wang et al., 2001a) though MT is not localized in the mitochondria (Zhou and Kang, 2000).

The accumulation of ROS in the mitochondria appears to be an important cellular event triggering apoptosis involved in the DOX-induced cardiac injury. Therefore, it is important to define the molecular mechanisms by which MT inhibits the accumulation of ROS in the mitochondria. Recent developments in proteomics have permitted robust investigations into the molecular mechanisms underlying cardiovascular disease and have allowed for identification of protein modifications (Arrell et al., 2001). Proteomics techniques also offer the ability to simultaneously monitor differential changes in protein expression in response to various stimuli and under different physiological and pathological conditions (Macri and Rapundalo, 2001). In previous studies proteomics approaches have been used to identify DOX-induced protein

changes in MCF-7 human breast cancer cells (Chen et al., 2002). Proteomics techniques would also offer a powerful approach to understanding molecular mechanisms of MT protection against DOX cardiotoxicity.

In the present study we used the unique cardiac-specific MT-TG mouse model in concert with expression proteomics approaches to identify differences in global proteomic profiles between the WT and MT-TG mice in their responses to DOX cardiotoxicity, focusing on the effect of MT on mitochondrial protection and thereby inhibition of myocardial oxidative injury. Our data indicate that cytochrome c oxidase subunit Va (CCO-Va) is among several proteins that are differentially expressed or modified in response to DOX treatment in the MT-TG mouse hearts relative to controls. Since CCO-Va is a critical component of the terminal enzyme of the mitochondrial electron transport chain, the results obtained suggest that the cardioprotective effect of MT may be related to an increased expression or a differential modification of CCO-Va.

Methods

Chemicals and reagents. Doxorubicin hydrochloride (DOX) was purchased from Sigma (St. Louis, MO). Immobiline pH gradient strips were from Amersham Biosciences (Uppsala, Sweden). Duracryl Tricine Chemistry gels and ampholytes were obtained from Genomic Solutions (Ann Arbor, MI). Sypro Ruby was purchased from Bio-Rad (Hercules, CA) and trypsin was from Promega (Madison, WI). Anti-CCO-Va monoclonal antibody was purchase from Molecular Probes (Eugene, OR) and HRP conjugated secondary antibody was purchased from Upstate Biotechnology (Waltham, MA). All other reagents were obtained from Sigma and were at least analytical grade.

Animals. Male FVB WT mice and cardiac-specific MT-TG mice (8-10 weeks) were maintained at the University of Louisville Research Resources Center at 22 °C with a 12-h light/dark cycle and were allowed free access to rodent chow and tap water. The cardiac-specific MT-TG mice were produced and characterized as previously reported (Kang et al., 1997). The transgenic founder mice were bred with WT mice of the same strain. Transgenic littermates were identified by a pigment transgene marker (dark eye and fur) that was coinjected with the MT transgene into the early embryo when the transgenic mice were produced. Transgenic and WT mice were randomly assigned to control or treatment groups and were treated intraperitoneally with either 0.9% NaCl or with DOX at a single dose of 20 mg/kg body weight. All animal procedures were approved by the Institutional Animal Care and Use Committee, which is certified by the American Association for Accreditation of Laboratory Animal Care.

Sample preparation. Three days after DOX treatment mice were sacrificed and the hearts were removed and homogenized in solubilization buffer containing 8 M urea, 2 M thiourea, 2% CHAPS, 65 mM dithiothreitol (DTT), 1% Zwittergent, and 1% protease inhibitor

cocktail. Homogenates were allowed to incubate at room temperature for 30 minutes and were then centrifuged twice at 14,000 x g for 15 minutes. The supernatant was then collected and the protein concentration of each sample was determined using the Bradford assay (Bio-Rad). Initial studies indicated considerable variations in protein levels among individual animals, thereby complicating data analysis. In order to eliminate the variations, three hearts from each treatment group were pooled to run the gel electrophoresis and imaging analysis, and 4 gel electrophoresis and analysis were conducted for each treatment group. The same experiment was repeated 3 times (a total of 9 mice and 12 gels for each treatment group).

Two-dimensional gel electrophoresis. First dimension isoelectric focusing (IEF) was performed using 18-cm immobilized pH gradient (IPG) strips with a pH range 3-10 using a passive in-gel rehydration method. Briefly, 400 μg protein samples from each experimental group (Con-WT, Con-TG, DOX-WT, DOX-TG) was diluted in a rehydration buffer containing 7 M urea, 2 M thiourea, 2% CHAPS, 65 mM DTT, 1% Zwittergent, 0.80% ampholytes pH 3-10, and 0.01% bromphenol blue to a volume of 400 μl and allowed to incubate at room temperature for 30 minutes to allow the samples to be fully solubilized. Following incubation, protein samples in rehydration buffer were added to IPG strips and the strips were allowed to rehydrate overnight at room temperature. IEF was performed at 5000 V for 24 h for a total of 100,000 Vh using a Genomic Solutions pHaser Isoelectric Focusing System. After IEF was completed, IPG strips were equilibrated for 15 minutes in equilibration buffer containing 45 mM Tris-HCl, pH 7.0, 6 M urea, 130 mM DTT, 30% glycerol, 1.6% SDS, and 0.002% bromphenol blue, followed by a second 15 minute incubation in the same buffer. The IPG strips were then equilibrated for an additional 15 minutes in the same buffer containing 4.5% iodoacetamide in place of DTT. Sodium dodecyl sulfate-polyacrylamide gel electrophoresis (SDS-PAGE) was performed on 18

cm IPG strips using 12.5% Duracryl Tricine Chemistry gels at 4 °C for 5 hours. Gels were then stained with Sypro Ruby and gel images were captured using the ProXPRESS 2D Proteomic Imaging System (Perkin Elmer Life Sciences, Boston, MA) with excitation and emission wavelengths of 480 nm and 620 nm, respectively.

Two-dimensional gel image analysis. Gels were matched and analyzed for protein expression using Investigator HT Analyzer software (Genomic Solutions). Prior to image analysis, Sypro Ruby stained gels were inverted so that the density of the fluorescent stained spots could be detected as dark protein spots on a light background. For each treatment group an analysis set containing eight gels (out of 12 gels) was created and protein spots on each gel were detected and the imaging was digitalized and statistically analyzed. A representative gel was presented as a reference gel for each treatment group. Protein spots in each gel were then automatically matched to corresponding protein spots in the reference gel and any incorrectly matched protein spots were corrected manually. Individual protein spot numbers were then synchronized to the corresponding protein spot number in the reference gel. An average mode of background subtraction was used to normalize the intensity volume of each spot for compatibility of intensity among gels. To accurately compare the measurements of protein spots across different gels and to correct for any protein loading differences a normalization volume was calculated for each protein spot in a given gel by dividing the volume of the individual spot by the total volume of all of the valid spots in the gel. Normalization volumes were then transferred to Microsoft Excel and an average normalization volume was determined for each protein spot in each treatment group. For each protein spot, three separate -fold changes were then calculated (Con-TG/Con-WT, DOX-WT/Con-WT, and DOX-TG/Con-TG).

JPET Fast Forward. Published on September 6, 2005 as DOI: 10.1124/jpet.105.089763
This article has not been copyedited and formatted. The final version may differ from this version.

Peptide mass fingerprinting. Protein samples of interest were excised from gels and taken for identification using peptide mass fingerprinting (PMF). Samples were excised from gels and digested with trypsin as described previously (Jensen et al., 1999). Initially, protein spots were minced into small gel pieces and incubated for 15 min in 50 mM NH_4HCO_3. Acetonitrile was then added to the gel suspension and the mixture was incubated for 15 min at room temperature. The wash buffer was then removed and the gel was dried via vacuum centrifugation. Subsequently, the gel pieces were rehydrated in 20 mM DTT in 100 mM NH_4HCO_3 and incubated at 56 °C for 45 min. The gel pieces were then incubated in 55 mM iodoacetamide in 100 mM NH_4HCO_3 at room temperature for 30 min in the dark. Following alkylation of the sulfhydryl groups, gel pieces were washed a second time in 50 mM NH_4HCO_3 and 50% acetonitrile for 15 minutes and dried via vacuum centrifugation. Finally, protein gel pieces were incubated in 25 ng/µl of modified trypsin at 37 °C overnight. Tryptic digests then underwent matrix-assisted laser desorption ionization time-of-flight (MALDI-TOF) peptide analysis.

Tryptic digests were initially mixed with an equal volume of α-cyano-4- hydroxy-trans-cinnamic acid (α-CN) matrix. The mixture was then deposited on a α-CN matrix surface and allowed to dry. The sample was subsequently washed with 5% formic acid to remove any water-soluble compounds. MALDI-TOF peptide fingerprint mass spectra were acquired with a TofSpec 2E MALDI/TOF mass spectrometer (Micromass, UK) with a nitrogen laser. Peptide masses acquired by MALDI-TOF peptide analysis were searched against a subset of mouse proteins in the National Center for Biotechnology Information (NCBI) protein database using the Mascot search engine (Matrix Science, London, UK) (www.matrixscience.com). The search was based on three assumptions. First, that the polypeptides are monoisotopic. Second, the peptides

may be oxidized at methionine residues. Third, that the peptides are carbamidomethylated at cysteine residues. Also, one missed trypsin cleavage and a mass tolerance of 100 ppm were allowed for matching the peptide mass values.

Two-dimensional gel electrophoresis linked immunoblot analysis. First dimension IEF was performed using 7-cm IPG strips with a pH range 4-7 as above. Five micrograms of protein sample from DOX-TG was diluted in rehydration buffer containing IPG buffer pH 4-7 in place of ampholytes pH 3-10 to a volume of 125 μl. As before, rehydrated sample was added to IPG strips and the strips were allowed to rehydrate overnight at room temperature. IEF was performed at 5000 V for 2 hr 40 min for a total of 8000 Vh. Strips were equilibrated as before and SDS-PAGE was performed using 17% Tris-glycine gels. Protein was then transferred to polyvinylidene difluoride (PVDF) membrane for immunoblot analysis. Non-specific binding was blocked via incubation of the membrane in blocking buffer (5% nonfat dry milk in Tris-buffered saline) for 2 hr followed by incubation at 4 °C overnight in primary antibody (monoclonal anti-cytochrome c oxidase subunit Va, 1:2000) diluted in blocking buffer. The membrane was washed in TBST (Tris-buffered saline, 1% Tween 20) and incubated for 2 hr at room temperature with HRP conjugated goat anti-mouse IgG (1:2000). The blot was then processed and visualized by chemiluminescence (Amersham Biosciences).

Statistical analysis: All data are expressed as mean ± SE (n=8). The data were analyzed according to a 2 X 2 factorial design. After a significant interaction was detected by the multi-way analysis of variance (ANOVA), the significance of the main effects was further determined. The level of significance was considered when $p<0.05$ as well as when a 2-fold difference, either increase or decrease, between the treated and control groups was detected.

Results

Under the treatment condition applied here, DOX induced dramatic morphological changes in the WT mouse heart including nuclear chromatin margination, severe mitochondrial swelling, cristae disappearance and matrix clearout. Serum creatine phosphokinase (CPK) activities were also significantly increased. In the MT-TG mice DOX-induced morphological alterations and elevation of serum CPK activities were significantly suppressed. The DOX cardiotoxic effects and the MT protection observed here (data not shown) were in a good agreement with that reported before (Kang et al., 1997; Sun et al., 2001).

Conventional two-dimensional gel electrophoresis (IEF/SDS-PAGE) was performed using total cardiac lysate to identify differences in proteomic profiles between the WT and MT-TG mouse hearts and their responses to DOX toxicity. The results presented in Fig. 1 show the effects of MT on DOX-induced changes in cardiac proteomic profiles. The gels were stained with Sypro Ruby to visualize proteins. Image analysis using Investigator HT Analyzer software revealed that 90 individual protein spots were differentially expressed ($p<0.05$ and a 2-fold or more difference, either increase or decrease, between the groups) in either WT or MT-TG mouse hearts in response to DOX treatment. Fold changes were calculated by dividing the average normalization volume of the spots from the eight DOX-treated gels by the average normalization volume of the spots from the eight control gels. Of these spots, 21 protein spots were increased and 18 were decreased in the WT mouse hearts (DOX-WT/Con-WT), but not changed in the MT-TG mouse hearts (DOX -TG/Con-TG). In the MT-TG mouse hearts 11 protein spots were increased and 10 were decreased, but not changed in the WT mouse hearts. Image analysis also revealed that 3 protein spots were increased in the WT mouse hearts while being decreased in the MT-TG mouse hearts following DOX treatment and that another 5 protein spots were decreased

in the WT mouse hearts while being increased in the MT-TG mouse hearts following DOX treatment. Another 13 proteins were increased and 9 proteins were decreased in both WT and MT-TG mouse hearts following DOX treatment. All of the 90 protein spots were analyzed by MALDI-TOF mass spectrometry and 18 were identified successfully (Fig 2). These proteins included those involved in cellular antioxidant defense, nuclear encoded subunits of the mitochondrial electron transport chain, enzymes involved in β-oxidation of fatty acids and glycolysis, and proteins involved in regulation of cardiac muscle contraction (Table 1).

The individual protein spot that showed the greatest change in staining intensity following DOX treatment was spot 3 (Fig. 3). Following DOX treatment, spot 3 was found to be dramatically increased in the MT-TG mouse hearts in comparison to the MT-TG controls whereas in the DOX-treated WT mouse hearts spot 3 was found to be decreased slightly in comparison to the WT control (Table 1). Peptide masses acquired from the mass spectrum of spot 3 matched 7 theoretical peptide mass values of tryptic digests of cytochrome c oxidase subunit Va (CCO-Va) (Fig. 4A) and demonstrated a 48% coverage of the sequence (Fig 4B). Interestingly, immunoblot analysis of the total proteins isolated from the hearts did not reveal significant difference in CCO-Va among the four treatment groups (data not shown). Subsequent MALDI-TOF mass spectrometry analysis of protein spots adjacent to spot 3 in DOX-treated transgenic heart 2D gels identified that spot 2 was also CCO-Va (Fig. 5A). Two-dimensional gel electrophoresis linked immunoblot analysis of CCO-Va in the DOX-treated MT-TG mouse hearts revealed two specific spots for CCO-Va (Fig. 5B). MALDI-TOF mass spectrometry analysis also identified that both of these spots were CCO-Va. The quantitative changes between the two spots were significantly different among the treatment groups, however, the combined total amounts of the two spots were not significantly different. In

particular, CCO-Va in spot 3 was significantly increased and in spot 2 was significantly decreased in response to DOX treatment in the MT-TG mouse hearts.

Discussion

DOX-induced cardiotoxicity is related to the accumulation of ROS generated from DOX metabolism in the heart. Both early studies (Bachur et al., 1977; Cova et al., 1992; Goormaghtigh et al., 1980) and recent studies using more advanced techniques (Kang et al., 1996; 1997; Sun et al., 2001; Wang et al., 2001a) have shown that ROS accumulation in mitochondria of cardiomyocytes is highly responsible for the oxidative damage to the heart. In particular, ROS accumulation in mitochondria triggers myocyte apoptosis (Kang et al., 2000; Wang et al., 2001a; 2001b). MT inhibits DOX-induced myocardial apoptosis (Kang et al., 2000; Wang et al., 2001a) as well as ROS accumulation in mitochondria (Wang et al., 2001a). However, MT is not localized in mitochondria in the heart (Zhou and Kang, 2000; Ye et al., 2001). An important question that needs to be addressed is how MT affects DOX-induced ROS accumulation in mitochondria.

DOX-induced mitochondrial ROS accumulation is related to the mitochondrial oxidative phosphorylation process. DOX has been shown to act as a redox cycling alternate electron acceptor and thereby leads to the uncoupling of mitochondrial oxidative phosphorylation (Wallace and Starkov, 2000). DOX is converted to reduced semiquinone free radical after accepting electrons from complex I of the mitochondrial respiratory chain (Davies and Doroshow, 1986). This semiquinone free radical intermediate is highly unstable and rapidly reacts with molecular oxygen to generate superoxide free radical with regeneration of intact DOX (Jung and Reszka, 2001). Furthermore, redox cycling of DOX in the mitochondria was shown to generate not only superoxide but also H_2O_2 and more importantly hydroxyl radical (Doroshow and Davies, 1986). The production and accumulation of ROS in the mitochondria is therefore thought to be a major mechanism leading to DOX-induced cardiotoxicity.

In mammals, mitochondrial oxidative phosphorylation is catalyzed by five membrane bound protein complexes, NADH-ubiquinol oxidoreductase (complex I), succinate-ubiquinol oxidoreductase (complex II), ubiquinol-cytochrome c oxidoreductase (complex III), cytochrome c oxidase (CCO) (complex IV), and ATP synthase (complex V). These protein complexes are composed of multiple subunits encoded by both mitochondrial DNA and nuclear DNA. The mitochondrion contributes thirteen of these subunits, whereas the remaining subunits (approximately 70) are encoded by nuclear DNA. Since MT is not localized in myocardial mitochondria (Zhou and Kang, 2000; Ye et al., 2001), it is likely that MT modifies mitochondrial proteins that are encoded by nuclear DNA. CCO-Va would be such a protein (Grossman and Lomax, 1997).

CCO (complex IV) is the terminal enzyme of the mitochondrial respiratory chain and as such catalyzes the transfer of electrons from reduced cytochrome c to molecular oxygen. CCO is the primary determinant of molecular oxygen consumption in the cell and is thought to play an important role in the regulation of energy production (Capaldi, 1990; Poyton and McEwen, 1996). In mammals, CCO is composed of 13 subunits; 3 mitochondrial-encoded subunits and 10 nuclear encoded subunits, some of which occur as tissue-specific isoforms (Grossman and Lomax, 1997). The three mitochondrial-encoded subunits compose the catalytic center of the enzyme and are essential and sufficient to carry out the catalytic function of CCO (Grossman and Lomax, 1997). The exact function of the nuclear encoded subunits of CCO has long been a topic of debate. Experimental studies, however, suggest that these nuclear encoded subunits are involved in the regulation of CCO activity, including the rate of respiration as well as the efficiency of proton translocation (Kadenbach, 2003). The nuclear encoded subunits of CCO,

including CCO-Va, are therefore thought to be of importance in the regulation of oxidative phosphorylation.

A specific function for CCO-Va has been shown in reconstituted CCO from bovine heart. The thyroid hormone 3,5-diiodothyronine was found to specifically bind to CCO-Va using the radioactive hormone [3-^{125}I]5-diiodothyronine (Arnold et al., 1998). This binding abolishes the allosteric inhibition of CCO activity by ATP and leads to stimulation of respiration (Arnold et al., 1998). Further function of CCO-Va in mitochondrial oxidative phosphorylation has yet to be determined and it is unknown whether CCO-Va is subjected to posttranslational modification in the heart. However, in the present study, the expression proteomic analysis indeed identified two different CCO-Va protein spots in the 2D gels. Interestingly, MT overexpression in the heart did not change the total concentrations of CCO-Va under the treatment with DOX relative to saline-treated controls, however, MT caused a shift of the dominant isoforms; enhanced one isoform and reduced the other. We postulate that this alteration would be due to a posttranslational modification of CCO-Va and that such modification could enhance the oxidative phosphorylation reaction thereby increasing the utilization of molecular oxygen and reducing the opportunity for the generation and accumulation of ROS in the mitochondria.

Besides the CCO-Va, which showed the most dominant change in the MT-TG mouse heart in response to DOX treatment, some other proteins also showed differential changes. The significance of these changes is subjected to further analysis. Further work is also necessary to elucidate the mechanism by which CCO-Va is modified by MT and the functional significance of this modification in protection from DOX cardiotoxicity. The present study demonstrates that modification of CCO-Va in the heart is likely involved in MT protection from DOX

cardiotoxicity, directing our future effort on the mechanistic understanding of MT modification of this protein and functional significance of the modification.

Acknowledgements

The authors thank Aisha Bagshaw and Johnny Morehouse for technical assistance, and Janice Scherzer and Daniel Wilkey for assistance in computational analysis of the data generated from 2D gel-electrophoresis.

References

Arnold S, Goglia F, Kadenbach B (1998) 3,5-Diiodothyronine binds to subunit Va of cytochrome-c oxidase and abolishes the allosteric inhibition of respiration by ATP. *Eur J Biochem* 252:325-330.

Arrell DK, Neverova I, Van Eyk JE (2001) Cardiovascular proteomics: evolution and potential. *Circ Res* 88:763-773.

Bachur NR, Gordon SL, Gee MV (1977) Anthracycline antibiotic augmentation of microsomal electron transport and free radical formation. *Mol Pharmacol* 13:901-910.

Capaldi RA (1990) Structure and function of cytochrome c oxidase. *Annu Rev Biochem* 59:569-596.

Chen ST, Pan TL, Tsai YC, Huang CM (2002) Proteomics reveals protein profile changes in doxorubicin-treated MCF-7 human breast cancer cells. *Cancer Lett* 181:95-107.

Cova D, De Angelis L, Monti E, Piccinini F (1992) Subcellular distribution of two spin trapping agents in rat heart: possible explanation for their different protective effects against doxorubicin-induced cardiotoxicity. *Free Radic Res Commun* 15:353-360.

Davies KJ, Doroshow JH (1986) Redox cycling of anthracyclines by cardiac mitochondria. I. Anthracycline radical formation by NADH dehydrogenase. *J Biol Chem* 261:3060-3067.

Doroshow JH, Davies KJ (1986) Redox cycling of anthracyclines by cardiac mitochondria. II. Formation of superoxide anion, hydrogen peroxide, and hydroxyl radical. *J Biol Chem* 261:3068-3074.

Ferrans VJ (1978) Overview of cardiac pathology in relation to anthracycline cardiotoxicity. *Cancer Treat Rep* 62:955-961.

Goormaghtigh E, Chatelain P, Caspers J, Ruysschaert JM (1980) Evidence of a complex between adriamycin derivatives and cardiolipin: possible role in cardiotoxicity. *Biochem Pharmacol* 29:3003-3010.

Grossman LI, Lomax MI (1997) Nuclear genes for cytochrome c oxidase. *Biochim Biophys Acta* 1352:174-192.

Jensen ON, Wilm M, Shevchenko A, Mann M (1999) Sample preparation methods for mass spectrometric peptide mapping directly from 2-DE gels. *Methods Mol Biol* 112:513-530.

Jung K, Reszka R (2001) Mitochondria as subcellular targets for clinically useful anthracyclines. *Adv Drug Deliv Rev* 49:87-105.

Kadenbach B (2003) Intrinsic and extrinsic uncoupling of oxidative phosphorylation. *Biochim Biophys Acta* 1604:77-94.

Kang YJ, Chen Y, Epstein PN (1996) Suppression of doxorubicin cardiotoxicity by overexpression of catalase in the heart of transgenic mice. *J Biol Chem* 271:12610-12616.

Kang YJ, Chen Y, Yu A, Voss-McCowan M, Epstein PN (1997) Overexpression of metallothionein in the heart of transgenic mice suppresses doxorubicin cardiotoxicity. *J Clin Invest* 100:1501-1506.

Kang YJ, Zhou ZX, Wang GW, Buridi A, Klein JB (2000) Suppression by metallothionein of doxorubicin-induced cardiomyocyte apoptosis through inhibition of p38 mitogen-activated protein kinases. *J Biol Chem* 275:13690-13698.

Macri J, Rapundalo ST (2001) Application of proteomics to the study of cardiovascular biology. *Trends Cardiovasc Med* 11:66-75.

Poyton RO, McEwen JE (1996) Crosstalk between nuclear and mitochondrial genomes. *Annu Rev Biochem* 65:563-607.

Sun X, Zhou Z, Kang YJ (2001) Attenuation of doxorubicin chronic toxicity in metallothionein-overexpressing transgenic mouse heart. *Cancer Res* 61:3382-3387.

Wallace KB, Starkov AA (2000) Mitochondrial targets of drug toxicity. *Annu Rev Pharmacol Toxicol* 40:353-388.

Wang GW, Klein JB, Kang YJ (2001a) Metallothionein inhibits doxorubicin-induced mitochondrial cytochrome c release and caspase-3 activation in cardiomyocytes. *J Pharmacol Exp Ther* 298:461-468.

Wang GW, Zhou Z, Klein JB, Kang YJ (2001b) Inhibition of hypoxia/reoxygenation-induced apoptosis in metallothionein-overexpressing cardiomyocytes. *Am J Physiol Heart Circ Physiol* 280:H2292-H2299.

Ye B, Maret W, Vallee BL (2001) Zinc metallothionein imported into liver mitochondria modulates respiration. *Proc Natl Acad Sci* 98:2317-2322.

Zhou Z, Kang YJ (2000) Immunocytochemical localization of metallothionein and its relation to doxorubicin toxicity in transgenic mouse heart. *Am J Pathol* 156:1653-1662.

Footnotes

Funding: Supported in part by NIH grants HL59225 and HL63760 (YJK), and an NIEHS training grant ES011564 (KEM). YJK is a Distinguished University Scholar of the University of Louisville.

KEM and WF contributed equally to this study.

Legends for Figures

Figure 1. Effects of MT on DOX-induced changes in cardiac protein profiles. Representative high resolution separation of global cardiac proteins isolated from WT or MT-TG (MT) in response to DOX treatment relative to controls using two-dimensional IEF/SDS-PAGE.

Figure 2. Two-dimensional electrophoresis global cardiac protein profiles in the DOX-treated MT-TG mouse heart. Proteins that were differentially expressed (2-fold difference, either increase or decrease) following DOX treatment in either WT or MT-TG hearts were identified by peptide mass fingerprinting. Numbers are shown for 18 individual protein spots that were successfully identified and their identities are disclosed in Table 1.

Figure 3. Close-up of protein spot 3. Following DOX treatment, protein spot 3 was dramatically increased in the MT-TG mouse heart and slightly decreased in the WT heart in comparison to controls, as shown in Table 1.

Figure 4. Identification of protein spot 3 as CCO-Va. A, Mass spectrum obtained by tryptic digestion and peptide mass fingerprinting of protein spot 3. B, Amino acid sequence of CCO-Va. The underline indicates that the peptides that were acquired from the mass spectrum of spot 3 matched the Mascot search engine analysis.

Figure 5. A, Two different spots (spots 2 and 3) were identified from the protein profiles of mouse hearts as CCO-Va. B, Total cardiac lysate from DOX-treated MT-TG mice was separated by two-dimensional gel electrophoresis, transferred to PVDF membrane, and probed with anti-CCO-Va monoclonal antibody. CCO-Va in spot 3 was significantly increased and in spot 2 was decreased.

JPET Fast Forward. Published on September 6, 2005 as DOI: 10.1124/jpet.105.089763
This article has not been copyedited and formatted. The final version may differ from this version.

Table 1. Differential protein profiles identified between MT-TG and WT mouse hearts in response to DOX treatment relative to controls.

Protein Name (NCBI Accession Number)	Spot Number	M_r[a] *kDa*	pI[a]	Con-TG/ Con-WT[b]	DOX-WT/ Con-WT[b]	DOX-TG/ Con-TG[b]	Functional Category
Ubiquinol-cytochrome C reductase subunit VI (gi17380333)	18	15.0 (13.5)	9.3 (9.1)	1.37	3.99 *	0.99	Respiratory chain Complex III
Tu translation elongation factor, mitochondrial (gi27370092)	84	48.4 (47.7)	6.6 (7.6)	1.17	2.71 *	1.39	Mitochondrial protein synthesis
Sarcalumenin (gi34328417)	124	59.6 (54.6)	6.0 (6.2)	1.92	3.92 *	1.33	Calcium handling
Nucleoside-diphosphate kinase B (gi6679078)	10	19.2 (17.4)	7.2 (6.9)	1.70	0.32 *	0.54	Nucleoside synthesis/ Transcription factor
ATP synthase, mitochondrial F0 complex, subunit d (gi51980458)	34	28.8 (18.8)	5.2 (5.5)	0.92	0.25 *	0.86	Respiratory chain Complex V
Aconitase 2, mitochondrial (gi18079339)	148	95.3 (86.1)	7.8 (8.0)	1.41	0.37 *	0.56	Citric acid cycle/ Mitochondrial DNA maintenance
Acyl-Coenzyme A dehydrogenase, very long chain (gi23956084)	150	72.3 (71.2)	8.1 (8.9)	0.80	0.48 *	0.88	β-Oxidation of fatty acids
Fatty acid binding protein 3 (gi6753810)	5	16.2 (14.8)	5.7 (6.1)	0.85	0.65	2.05 *	Long-chain fatty acid metabolism
Peroxiredoxin 6 (gi3219774)	56	30.8 (24.9)	6.1 (5.7)	1.09	1.47	2.10 *	Cellular antioxidant defense
Myoglobin (gi21359820)	9	17.9 (17.1)	7.0 (7.0)	1.06	0.77	0.07 *	Oxygen handling
Pyruvate dehydrogenase beta (gi18152793)	73	40.0 (39.2)	5.4 (6.4)	0.96	1.11	0.39 *	Metabolism/ Energy pathways
Enolase 3 (gi6679651)	129	52.3 (47.3)	6.7 (6.7)	1.21	0.63	0.17 *	Glycolytic enzyme
Vimentin (gi2078001)	114	59.4 (51.6)	4.7 (5.0)	1.37	4.00 *	0.41 *	Type III intermediate filament
Cytochrome c oxidase subunit Va (gi6680986)	3	14.5 (16.2)	5.0 (6.1)	0.92	0.42 *	30.43 *	Respiratory chain Complex IV
Cardiac Troponin T isoform A1b (gi1161066)	79	45.2 (34.9)	5.4 (5.2)	0.84	0.27 *	2.55 *	Cardiac muscle contraction
Alpha-tropomyosin (gi20178271)	71	36.1 (32.7)	4.3 (4.7)	1.01	0.48 *	0.19 *	Cardiac muscle contraction
Acyl-CoA dehydrogenase mitochondrial precursor (LCAD) (gi32130423)	99	46.0 (48.3)	6.9 (8.5)	0.62	0.12 *	0.07 *	β-Oxidation of fatty acids
Aldolase 1 (gi42490830)	187	42.1 (39.7)	8.7 (8.5)	0.75	0.09 *	0.22 *	Glycolytic enzyme

[a] Theoretical values for M_r and pI are shown in parenthesis and were obtained from the National Center for Biotechnology Information (NCBI) protein database. [b] Fold changes were calculated by dividing the average normalization volume of the spots from DOX-treated gels by the average normalization volume of the spots from the control gels. * Significant changes were identified when a 2-fold change in the staining intensity (2-fold difference, either increase or decrease) was observed.

JPET Fast Forward. Published on September 6, 2005 as DOI: 10.1124/jpet.105.089763
This article has not been copyedited and formatted. The final version may differ from this version.

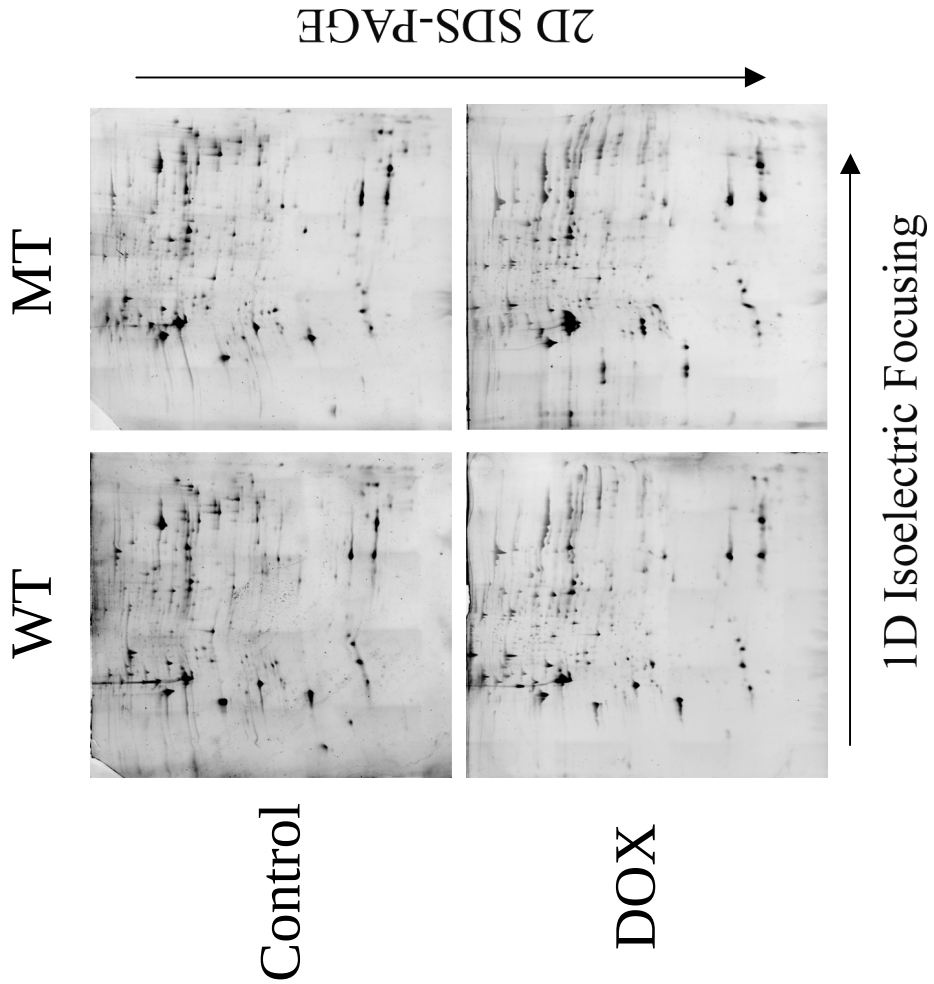

Figure 1

Figure 2

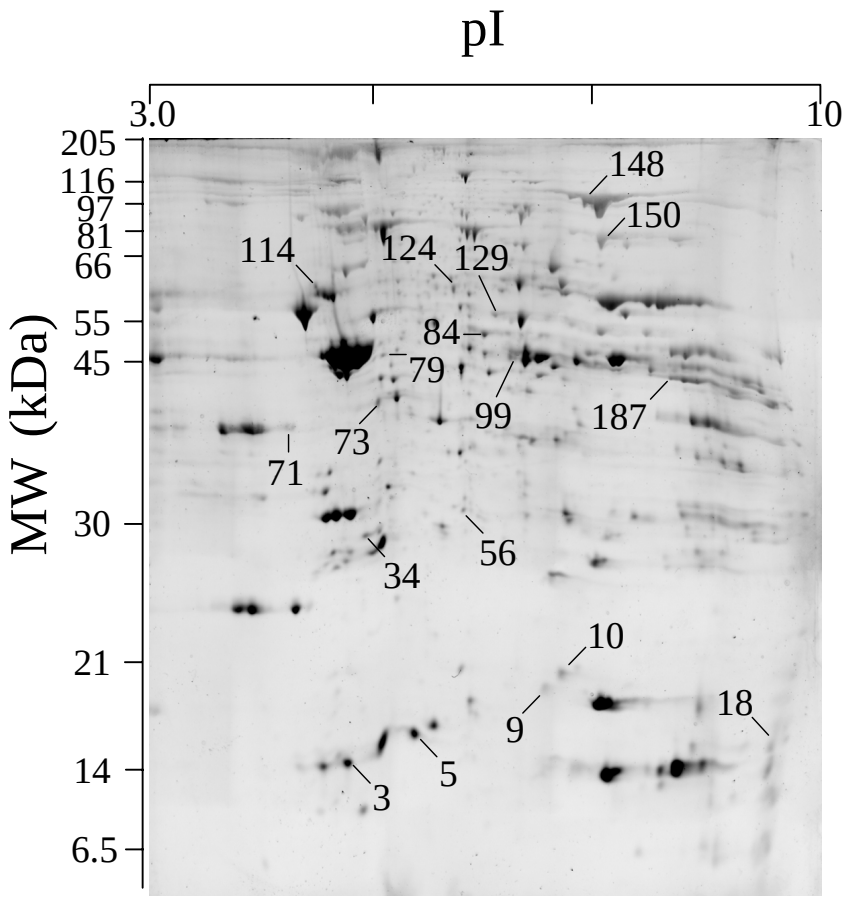

Figure 3

Figure 4

A

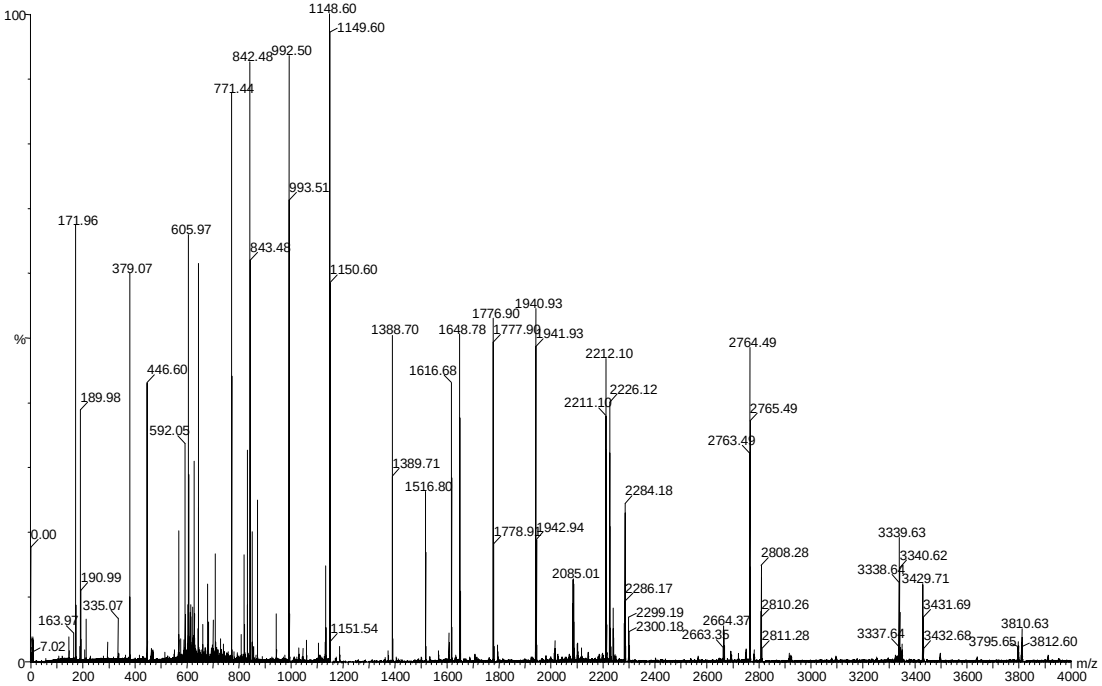

B

```
  1 MLAAALRRCT AAAAARGLLH PASAPSPAAA VCSIRCYSHG SHETDEEFDA
 51 RWVTYFNKPD IDAWELRKGM NTLVGYDLVP EPKIIDAALR ACRRLNDFAS
101 AVRILEVVKD KAGPHKEIYP YVIQELRPTL NELGISTPEE LGLDKV
```

Figure 5